Combined static potentials for confinement of neutral species

Leonardo Ricci,* Davide Bassi, and Andrea Bertoldi†
Dipartimento di Fisica, Università di Trento, I-38050 Trento-Povo, Italy
(Received 31 May 2007; published 31 August 2007)

We discuss the general problem of generating confining potentials for neutral matter by combining different kinds of static forces. The interactions taken into account are those having a linear or quadratic dependence on the modulus of an irrotational and solenoidal field. Particular attention is devoted to the combination of electric and magnetic forces for paramagnetic species. In this case, tight confinement can be achieved by enhancing and balancing the field gradients. Combined potentials turn out to be conveniently generated by configurations based on high permeability materials. Feasibility of combined electric-magnetic traps and guides for neutral alkali-metal atoms is discussed.

DOI: 10.1103/PhysRevA.76.023428 PACS number(s): 32.80.Pj, 07.55.Db, 39.25.+k, 85.90.+h

I. INTRODUCTION

In the last two decades, confining potentials relying upon suitably shaped magnetic fields have been exploited as an extremely reliable tool for the manipulation of cold neutral matter.

Magnetic fields are used to generate both trapping [1] and guiding potentials [2–5]. In this last context, tight confinement along single or more dimensions often constitutes the key requirement, for example, to achieve quantum propagation of atomic de Broglie waves [6].

The goal of tight confinement has been mainly pursued by miniaturizing the setups [7–11], especially with regard to atom guiding. In this framework, the magnetic field is usually generated by current-carrying wires lithographically patterned on a substrate [12–15]. Recently, the realization of a superconducting atom chip has been reported [16].

Another approach aiming to generate tight potentials relies on the utilization of ferromagnetic structures [17–21]. This solution exploits the property of high permeability materials (μ-metals) to conduct and concentrate the magnetic field flux. Related to this, μ-metal poles act as equipotential surfaces for the scalar potential describing the magnetic field in a current-free region. However, since it is no longer possible to apply the superposition principle inherent in the Biot-Savart law, the design of magnetic field source configurations containing μ-metals is far more demanding than in the case of setups entirely based on current-carrying wires.

In this paper we discuss how to create confining potentials for neutral particles by combining static magnetic, electric, and gravitational fields. The core idea is to remove the constraint of working in a minimum of a single potential (typically the magnetic field modulus) by compensating the resulting force with an additional force. To generate the confining potentials, we consider here the interactions proportional to the first or second power of the modulus of a solenoidal (divergence-free) and irrotational (rotation-free) field, such as the static electric or magnetic field. More in detail, the interactions considered are as follows: the magnetic force acting on a paramagnetic species, the diamagnetic interaction, the quadratic Stark interaction, and finally, under very ordinary conditions, the standard uniform gravitational potential.

Combinations of static electric, magnetic, and gravitational fields were first discussed by Ketterle and Pritchard [22] who demonstrated that it is impossible to trap ground-state particles at rest using these configurations. To overcome this limit, particles are here supposed to be in a metastable, low-field seeking state for at least one of the component potentials.

The use of combined potentials can be advantageous in many respects. For example, field gradients and curvatures can be strongly enhanced so as to yield tighter confinement. In addition, the utilization of electric fields to realize combined potentials allows for a great versatility. Moreover, a trap can be located in a region of nonvanishing magnetic field, thus preventing confined atoms to undergo Majorana spin flips. The method can be employed to design confining potentials suitable to observe and possibly exploit Feshbach resonances [23]. Finally, the combined potential approach simplifies the design of confining configurations using μ-metals.

Combined confining potentials exploiting magnetism and gravitation have been used to achieve magnetic levitation of macroscopic objects [24,25]. Combined magnetic-electric one-dimensional (1D) quantum wires [26,27] and ring trap [28] have been proposed. The quadratic Stark interaction has been used to modify a linear magnetic guide [29], whereas a gravitomagnetic trap has been employed to produce Bose-Einstein condensates at extremely low temperatures [30]. Moreover, confining systems based on combinations of dipole forces [31] with the gravitational or the quadratic Stark interaction have been proposed [32,33] and demonstrated [34]. Finally, a combination of a laser guide and a magnetic lens to transport a cold atomic cloud has been proposed [35].

The paper is structured as follows. In Sec. II, the formalism adopted to treat combined potentials is introduced, while the topic of tight confinement is discussed in Sec. III. Section IV deals with the more physical aspects, including possible confining combinations. In Sec. V, the combination of electric and magnetic fields for confinement of paramagnetic species, such as neutral alkali-metal atoms, is discussed; con-

*ricci@science.unitn.it
†Present address: Dipartimento di Fisica, Università di Firenze, I-50019 S. Fiorentino-Firenze, Italy.

figurations having cylindrical or translational-planar symmetry are treated in depth. Finally, as an example, the design of a possible electric-magnetic linear guide for neutral atoms is presented.

II. SECOND-ORDER TAYLOR EXPANSION OF THE MODULUS AND THE MODULUS SQUARE OF A SOLENOIDAL AND IRROTATIONAL FIELD

In a neighborhood of a point, which is set as origin, a generic vectorial field $\boldsymbol{C}$ can be expanded up to the second order in the coordinates in the following way:

$$C_i = C_{i0} + \frac{\partial C_i}{\partial r_j} r_j + \frac{1}{2}\frac{\partial^2 C_i}{\partial r_j\,\partial r_k} r_j r_k + O(r^3), \tag{1}$$

where $O(r^3)$ groups terms of order higher than two. In the previous expression and henceforth, the partial derivatives are supposed to be evaluated in the origin; moreover, summation over repeated indices is implicitly assumed, with each index running on the three Cartesian coordinates. The modulus square of the field can be derived from Eq. (1) up to the second order,

$$|\boldsymbol{C}|^2 = |\boldsymbol{C}_0|^2 + 2C_{i0}\frac{\partial C_i}{\partial r_j} r_j + \left(C_{i0}\frac{\partial^2 C_i}{\partial r_j\,\partial r_k} + \frac{\partial C_i}{\partial r_j}\frac{\partial C_i}{\partial r_k}\right) r_j r_k + O(r^3). \tag{2}$$

In the following, a nonvanishing field modulus in the origin $|\boldsymbol{C}_0|$ is considered. It is convenient to define the gradientlike first-order tensor (vector) γ_j and the curvaturelike second-order tensor (matrix) ζ_{jk} as

$$\gamma_j \equiv \frac{C_{i0}}{|\boldsymbol{C}_0|}\frac{\partial C_i}{\partial r_j} = \frac{\boldsymbol{C}_0}{|\boldsymbol{C}_0|}\frac{\partial \boldsymbol{C}}{\partial r_j}, \tag{3}$$

$$\zeta_{jk} \equiv \frac{C_{i0}}{|\boldsymbol{C}_0|}\frac{\partial^2 C_i}{\partial r_j\,\partial r_k} + \frac{1}{|\boldsymbol{C}_0|}\frac{\partial C_i}{\partial r_j}\frac{\partial C_i}{\partial r_k}. \tag{4}$$

In this way, Eq. (2) becomes

$$|\boldsymbol{C}|^2 = |\boldsymbol{C}_0|^2 + 2|\boldsymbol{C}_0|\gamma_j r_j + |\boldsymbol{C}_0|\zeta_{jk} r_j r_k + O(r^3). \tag{5}$$

An analogous expression for the modulus of the field can be derived as

$$|\boldsymbol{C}| = |\boldsymbol{C}_0| + \gamma_j r_j + \frac{1}{2}\left(\zeta_{jk} - \frac{\gamma_j\gamma_k}{|\boldsymbol{C}_0|}\right) r_j r_k + O(r^3). \tag{6}$$

By defining a new second-order matrix ξ as

$$\xi_{jk} \equiv \zeta_{jk} - \frac{\gamma_j\gamma_k}{|\boldsymbol{C}_0|}, \tag{7}$$

or equivalently

$$\xi_{jk} \equiv \frac{C_{i0}}{|\boldsymbol{C}_0|}\frac{\partial^2 C_i}{\partial r_j\,\partial r_k} + \frac{1}{|\boldsymbol{C}_0|}\left(\frac{\partial C_i}{\partial r_j}\frac{\partial C_i}{\partial r_k} - \gamma_j\gamma_k\right), \tag{8}$$

Eq. (6) can be written as

$$|\boldsymbol{C}| = |\boldsymbol{C}_0| + \gamma_j r_j + \frac{1}{2}\xi_{jk} r_j r_k + O(r^3). \tag{9}$$

The vector $\boldsymbol{\gamma}$ and the matrix ξ are the gradient and the Hessian of the modulus of the field $\boldsymbol{C}$, respectively. The gradient and the Hessian of the modulus square are instead $2|\boldsymbol{C}_0|\boldsymbol{\gamma}$ and $2|\boldsymbol{C}_0|\zeta$, respectively.

In the Appendix it is shown that, if $\boldsymbol{C}$ is solenoidal and irrotational, then both ζ and ξ have non-negative trace, thus preventing the corresponding eigenvalues from being simultaneously negative, whatever the value of the gradientlike vector $\boldsymbol{\gamma}$. Each eigenvalue is equivalent to the curvature of the potential along the direction determined by the corresponding eigenvector.

In the case of $\boldsymbol{\gamma}=0$, this statement concerning the eigenvalues is a consequence of Earnshaw's theorem (see, for example, Ref. [36]), according to which the modulus of a solenoidal and irrotational field cannot have a maximum within a homogeneous medium. Earnshaw's theorem is indeed more general, as it deals also with cases in which the curvaturelike matrices are identically zero. The trace property, however, holds for any value of $\boldsymbol{\gamma}$, and it is thus applicable for potentials resulting as the sum of different contributions, each proportional to the modulus or the modulus square of a solenoidal and irrotational field.

III. TIGHT CONFINEMENT VIA GRADIENT ENHANCEMENT AND COMPENSATION

Once the total gradient is zero, the goal is to make each eigenvalue of the combined Hessian matrix non-negative and, possibly, as large as possible.

Let us first consider a single component potential. Neglecting momentarily the proportionality factor a, the Hessian matrix is ξ or $2|\boldsymbol{C}_0|\zeta$, depending on whether the potential is proportional to the modulus of a field $\boldsymbol{C}$ or its square, respectively. Both the Hessian matrices are given by the sum of two contributions [see Eq. (4) and Eq. (8)], one proportional to the spatial second derivatives (curvatures) of the field components and the other proportional to the products of the spatial first derivatives (gradients). As shown in the Appendix, the contribution to the trace by the terms containing the field curvatures is equal to zero: terms of this kind create saddle potentials, whose nontrapping sides are then to be compensated for. On the other hand, the contribution to the Hessian matrix by the terms containing the field gradients is always non-negative definite. These statements can be generalized to the case of a combined potential, leading to the conclusion that only terms containing the field gradients and belonging to potentials with positive coefficients a can make each eigenvalue of the overall Hessian matrix non-negative. Consequently, pursuing a tight confinement requires the maximization of these terms.

A first way to enhance the terms of the matrix ξ or $2|\boldsymbol{C}_0|\zeta$ that contain the field gradients is to reduce the bias field strength, as it results from Eq. (4) and Eq. (8). This fact is exploited, for example, in the Ioffe-Pritchard traps [37,38] in order to vary the radial curvature of the potential. The bias field, however, cannot be set arbitrarily small: its reduction amplifies the harmful effects for the trapped species stirred up by field fluctuations [39]. Moreover, higher-order terms in the Taylor expansion of the potential, and thus nonlinearities, can become significant.

The second, and safest, way to yield tighter confinement is therefore to directly enhance the field gradient terms ($\partial C_i/\partial r_j$). This goal has yet to comply with the requirement of vanishing gradient $\boldsymbol{\gamma}$ for the confining potential. Interestingly, in case of a single potential, this can be satisfied only by setting the three gradient vectors $\partial \boldsymbol{C}/\partial r_j$ ($j=1, 2, 3$) orthogonal to the bias field in the trap center $\boldsymbol{C}_0$, as it follows from Eq. (3). A remarkable consequence is that the Ioffe-Pritchard trap turns out to be the only possible cylindrically symmetric trapping configuration with a nonzero field minimum.

The constraint on $\boldsymbol{\gamma}$ for a single potential can be overcome by using an additional potential. In general, this additional potential will have nonzero curvatures so that its shape must be carefully chosen depending on the eigenvalues of the Hessian of the starting potential. A convenient situation is given when the additional potential is flat and thus only compensates for the gradient contributions given by the former one without perturbing its curvature terms.

An important example of an additional, flat potential is provided by uniform gravity (see Sec. IV). However, the slope $\boldsymbol{\gamma}$ is in this case fixed, as it depends exclusively on the gravity acceleration g and the mass m of the trapped species. This poses limits to the design of trapping configurations [40]. Nevertheless, gravity makes up an important candidate for combined confining potentials. Using a combined gravitomagnetic trap we obtained the levitation of a cloud of cold rubidium atoms. This experiment, which will be reported on in a separate paper, uses a magnetic field having a cylindrical symmetry. The field is characterized by a bias value of 0.5 G, an axial gradient of -15.4 G/cm, and an axial curvature of 90 G/cm^2. For ^{87}Rb atoms being in the $^2S_{1/2}$, $F=2$, $m_F=2$ hyperfine state, this gradient exactly compensates the weight force.

IV. COMBINED POTENTIALS

We consider a combined potential U as the sum of different contributions U_n,

$$U=\sum_n U_n,$$

each proportional to the first or the second power of the modulus of a solenoidal and irrotational field $\boldsymbol{C}_n$,

$$U_n = a_n|\boldsymbol{C}_n|^{\varepsilon_n}, \tag{10}$$

where the coefficients a_n are suitable proportionality constants and each ε_n is equal to 1 or 2. The gradient of the overall potential at the origin is then given by

$$\boldsymbol{\nabla} U = \sum_n a_n\varepsilon_n|\boldsymbol{C}_{n0}|^{\varepsilon_n-1}\boldsymbol{\gamma}_n,$$

whereas the Hessian is

$$\frac{\partial^2 U}{\partial r_j\,\partial r_k} = \sum_n a_n\varepsilon_n|\boldsymbol{C}_{n0}|^{\varepsilon_n-1}(\kappa_n)_{jk},$$

where, for each n,

$$\kappa \equiv \begin{cases} \xi & \text{if } \varepsilon=1, \\ \zeta & \text{if } \varepsilon=2. \end{cases}$$

Imposing U to have a minimum requires the gradient of U to vanish and, as a necessary condition, the trace of the total Hessian, or equivalently the Laplacian of U, to be nonnegative,

$$\nabla^2 U = \sum_n a_n\varepsilon_n|\boldsymbol{C}_{n0}|^{\varepsilon_n-1}\,\mathrm{Tr}\,\kappa_n \geq 0.$$

As shown in Sec. II, for each n it holds Tr $\kappa_n \geq 0$. Consequently, a minimum in a combined potential is achievable if there is at least one *attractive* potential, i.e., characterized by a positive coefficient a in Eq. (10); atoms (or molecules) behave as *low-field seekers* (LFS). An immediate consequence of this last statement is that no combination of static electric, magnetic, or gravitational fields can be used to trap ground-state particles, which, as known, are *high-field seekers* (HFS). This is in agreement with the results reported in [22]. The requirement of the particle being "quasistatically" LFS eventually calls for the validity of the adiabatic approximation.

The possible attractive potentials are the paramagnetic interaction for LFS described by $\mu|\boldsymbol{B}|$, where μ represents the modulus of the magnetic dipole moment, and the diamagnetic interaction $-\chi|\boldsymbol{B}|^2/2$ for particles having a negative susceptibility χ. These two forces are virtually mutually exclusive. Nonattractive components to yield combined potentials are then the quadratic Stark interaction $-\alpha|\boldsymbol{E}|^2/2$, where α is the static dipole polarizability, and the uniform gravitational field. Actually, this last potential is not proportional to the modulus of any solenoidal and irrotational field. Still, it can be treated in the very same way as the others provided that the field is uniform. To demonstrate it, let $\boldsymbol{C}_G$ be a divergence- and rotation-free field defined as

$$\boldsymbol{C}_G = U_{G0}\hat{\mathbf{z}} + mg\left(-\frac{1}{2}x\hat{\mathbf{x}} - \frac{1}{2}y\hat{\mathbf{y}} + z\hat{\mathbf{z}}\right),$$

where U_{G0} represents a suitable offset value, m the particle mass and g the gravity acceleration. Its modulus is

$$|\boldsymbol{C}_G| = U_{G0} + mgz + \frac{m^2g^2}{8U_{G0}}(x^2+y^2) + O(r^3).$$

The last expression corresponds to the standard uniform gravitational potential with acceleration directed along $-\hat{\mathbf{z}}$, provided that

$$U_{G0} \gg mg\ell,$$

where ℓ is the size of the region of interest (i.e., the confinement region).

To sum up, the possible combined potentials are the following:

(i) paramagnetic (LFS) species,

TABLE I. Parameter Γ_0, defined in Eq. (13a), for the alkali-metal atoms. Values are in $(\mathrm{kV/cm})^2/\mathrm{G}$.

Li[a]	Na[b]	K[b]	Rb[b]	Cs[b]	Fr[b]
68.51(4)	69.2(1)	38.8(1)	35.31(7)	28.1(1)	35.4(3)

[a]Reference [43].
[b]Reference [44].

$$U = \mu|\boldsymbol{B}| - \frac{1}{2}\alpha|\boldsymbol{E}|^2 + mgz; \tag{11}$$

(ii) diamagnetic species with $\chi < 0$,

$$U = \frac{1}{2}|\chi||\boldsymbol{B}|^2 - \frac{1}{2}\alpha|\boldsymbol{E}|^2 + mgz. \tag{12}$$

V. COMBINED POTENTIALS FOR PARAMAGNETIC SPECIES

In this section, we consider combinations of magnetic, electric, and gravitational potentials for paramagnetic species, and in particular for neutral alkali-metal atoms. Because of their practical importance, the discussion is focused on configurations with cylindrical or translational-planar symmetry.

Defining the quantities Γ and G as

$$\Gamma \equiv \frac{2\mu}{\alpha}, \tag{13a}$$

$$G \equiv \frac{mg}{\mu}, \tag{13b}$$

Eq. (11) can be rewritten as follows (henceforth we take z to be the vertical coordinate):

$$U = \frac{\alpha}{2}[\Gamma(|\boldsymbol{B}| + Gz) - |\boldsymbol{E}|^2]. \tag{14}$$

Depending on the total angular-momentum quantum number m_F and the Landé factor g_F of the atomic state, one has $\Gamma = m_F g_F \Gamma_0$, where the parameter Γ_0 is defined as $\Gamma_0 \equiv 2\mu_B/\alpha$. It is important to note that Eq. (11) holds if the quadratic Stark interaction does not mix hyperfine levels. For the ${}^2S_{1/2}$ state of alkali-metal atoms this condition is fulfilled, since the tensor polarizability α_2 is zero [41,42]. The value of the parameter Γ_0 for these atoms is reported in Table I. Given the atomic mass m_a of an isotope of interest, the value of the parameter G is given by $m_a \times 0.177$ G/cm.

Besides curvatures, two fundamental parameters that characterize any confining potential are depth and size. Depth is defined as the minimum kinetic energy necessary to escape a potential. In the case of a paramagnetic species, a magnetically confined particle can escape the potential either kinetically (the particle crosses the potential-well borders) or in consequence of a Majorana spin flip (the particle reaches a region where $B \sim 0$). As a result, if there exist zeroes of the magnetic field in the potential well, the general expression for the depth is

$$\frac{U_D}{\mu} = \min\left(\frac{|\boldsymbol{E}(0)|^2 - |\boldsymbol{E}(\boldsymbol{r}_0)|^2}{\Gamma} - |\boldsymbol{B}(0)| + Gz\right)_{\{r_0\}}, \tag{15}$$

where $|\boldsymbol{E}(0)|^2$ and $|\boldsymbol{B}(0)|$ are the electric field modulus square and the magnetic field modulus at the confinement center (taken as origin), whereas $\{\boldsymbol{r}_0\}$ corresponds to the set of points at which the magnetic field vanishes (locus of the zeroes).

In order to establish whether confinement occurs at a given point, it is sufficient to know the bias values, gradients and curvatures of the different fields in that point. On the other hand, the determination of the locus of the zeroes of $|\boldsymbol{B}|$, and thus of depth and size of the combined potential, generally requires the knowledge of higher-order terms of the Taylor expansion of the component fields.

A. Cylindrical symmetry

In this section, field source distributions having cylindrical symmetry are considered. Due to the presence of the gravitational field, the vertical axis (z axis) must be necessarily taken as the symmetry axis. In a neighborhood of a point on this axis, which is taken as the origin, the Taylor expansion for the magnetic field is determined up to the second order by three parameters: the bias field B_0, which is supposed to be strictly positive ($B_0 > 0$), the axial field gradient B', and the axial field curvature B'' ($r \equiv \sqrt{\rho^2 + z^2}$),

$$B_\rho = -\frac{1}{2}B'\rho - \frac{1}{2}B''\rho z + O(r^3), \tag{16a}$$

$$B_z = B_0 + B'z + \frac{1}{2}B''\left(z^2 - \frac{\rho^2}{2}\right) + O(r^3). \tag{16b}$$

The magnetic field modulus is

$$|\boldsymbol{B}| = B_0 + B'z + \frac{1}{2}B''z^2 + \frac{1}{4}\left(\frac{B'^2}{2B_0} - B''\right)\rho^2 + O(r^3).$$

Similar expressions can be derived for the electric field: in a neighborhood of the origin, the electric field modulus square is

$$E^2 = E_0^2 + 2E_0E'z + \frac{1}{2}(2E'^2 + 2E_0E'')z^2 + \frac{1}{4}(E'^2 - 2E_0E'')\rho^2 + O(r^3), \tag{17}$$

where E_0 represents the bias field (not necessarily positive), E' represents the axial field gradient, and E'' represents the axial field curvature.

The equations and inequalities relating to the different field parameters can be more easily handled by introducing three adimensional parameters s, ε, and ε',

$$s \equiv 2B_0B''/B'^2, \tag{18a}$$

$$\varepsilon \equiv \frac{\Gamma B'^2}{4B_0E'^2}, \tag{18b}$$

$$\varepsilon' \equiv \frac{\Gamma B'' - 2E_0E''}{2E'^2}. \tag{18c}$$

We impose the origin of the coordinates to coincide with the minimum of the combined confining potential described by Eq. (14). Confinement occurs only if the overall gradient vanishes,

$$2E_0E' = \Gamma(B' + G). \tag{19}$$

Another necessary condition is that the magnetic curvature is different from zero, or equivalently

$$s \neq 0. \tag{20}$$

The radial and axial curvatures of the combined potential at the origin (trap bottom) are expressed as follows:

$$\frac{\partial^2 U}{\partial x^2} = \frac{\partial^2 U}{\partial y^2} = \mu \frac{B'^2}{B_0} \frac{\varepsilon - \varepsilon' - \frac{1}{2}}{4\varepsilon}, \tag{21a}$$

$$\frac{\partial^2 U}{\partial z^2} = \mu \frac{B'^2}{B_0} \frac{\varepsilon' - 1}{2\varepsilon}. \tag{21b}$$

Therefore, provided that the conditions of Eqs. (19) and (20) are satisfied, confinement occurs if

$$\varepsilon - \frac{1}{2} > \varepsilon' > 1. \tag{22}$$

Using Eqs. (19) and (22), it is possible to choose the parameter triplet $\{E_0, E', E''\}$, that describes the electric field, once the magnetic triplet $\{B_0, B', B''\}$ is known, and vice versa.

It is interesting to note that, if the magnetic field is assigned *a priori* along with the two parameters ε and ε', the trap stiffness at the origin depends on both the magnetic field strength and gradient but not on its curvature. However, this last quantity, or equivalently the parameter s, codetermines the zeroes of the magnetic field and consequently size and depth of the spin-flips-free trapping region: using Eq. (16a) and (16b) and assuming the terms of order higher than two in the Taylor expansion of the magnetic field to be negligible in a sufficiently large neighborhood of the origin, it is straightforward to see that a cylindrically symmetric magnetic field described by a triplet $\{B_0, B', B''\}$ always vanishes either on two axial points (if $s \leq 1$) or on a ring (if $s \geq 1$). Some algebra provides the following:

(i) $s \leq 1 \Rightarrow$

$$\rho_0 = 0, \quad z_0 = -\frac{B'}{B''}(1 \pm \sqrt{1-s});$$

(ii) $s \geq 1 \Rightarrow$

$$\rho_0 = \left|\frac{B'}{B''}\right| \sqrt{2(s-1)}, \quad z_0 = -\frac{B'}{B''}.$$

Here, ρ_0 and z_0 represent the coordinates of the zeroes of the magnetic field. The case with $s \geq 1$ is at the basis for time-orbiting magnetic ring traps recently proposed [45] and implemented [46]. If $s=1$ the two axial zero points as well as the ring collapse to a single axial point placed at $z_0 = -B'/B''$.

As an example, Fig. 1 shows a combined trap for rubidium atoms. The parameter triplet for the electric field was determined on the basis of the magnetic field triplet and setting $\varepsilon=21$, $\varepsilon'=20$. The resulting combined potential, evaluated by assuming $\mu=\mu_B$ (Bohr's magneton), is shown in Fig. 1(c); it corresponds to a trap centered at the origin. The depth of the spin-flips-free trapping region is about $30 k_B \times \mu\mathrm{K}$, whereas its size is of the order of 0.5 mm. Both the electric and the magnetic field presented in this example are achievable by conventional techniques.

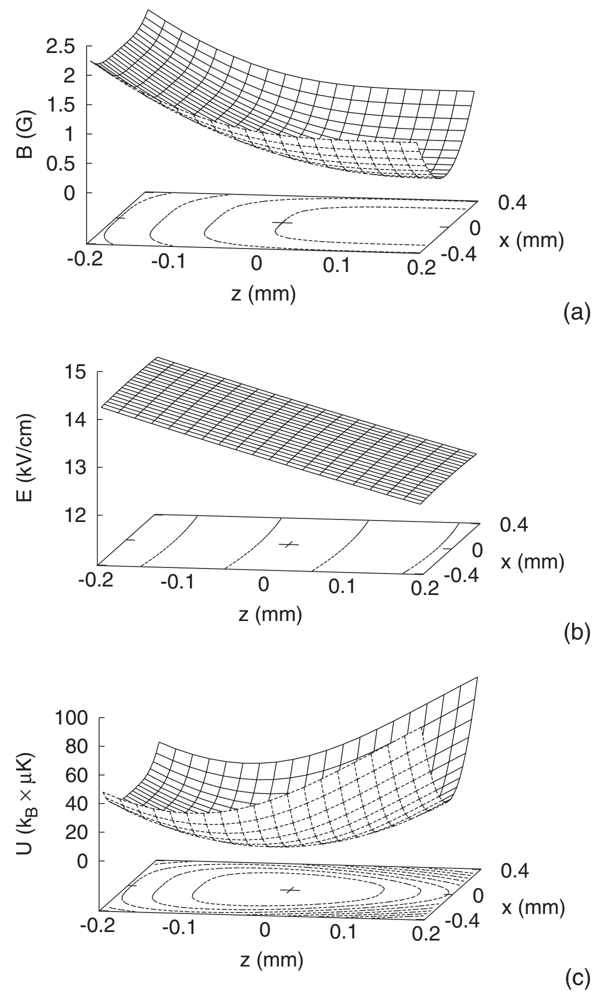

FIG. 1. Confining, cylindrically symmetric combined potential (c) for rubidium atoms having $\mu=\mu_B$. The potential is given by the difference of two contributions, the first (a) proportional to the modulus of a magnetic field characterized at the origin by the triplet $\{0.5\ \mathrm{G},\ -50\ \mathrm{G/cm},\ 2500\ \mathrm{G/cm^2}\}$ ($s=1$), and the second (b) proportional to the modulus square of an electric field ($\{13.3\ \mathrm{kV/cm},\ -45.8\ \mathrm{kV/cm^2},\ 158\ \mathrm{kV/cm^3}\}$ at the origin). The graphs are calculated in the plane $y=0$.

B. Translational-planar symmetry

In this section, field source distributions having both translational and planar symmetry are discussed. This geometry is typical of several atom guiding experiments.

First, let y be the translational (and horizontal) symmetry axis. Second, we impose an additional, planar symmetry for the system and assume the related symmetry plane to contain the y axis. Due to the presence of the gravitational field, this symmetry plane must necessarily coincide with the plane π_{yz} (as above, z is taken as the vertical axis). The discussion can be then restricted to the plane π_{xz}.

Two cases can be distinguished, depending on whether the field sources are specularly identical or, alternatively, *conjugated* under specular reflection. In the former case (henceforth case I), the magnetic field, being a pseudovector, transforms as

$$B_x(-x,\ z) = B_x(x,\ z),$$

$$B_z(-x,\ z) = -B_z(x,\ z),$$

whereas in the latter case (henceforth case II) as

$$B_x(-x,\ z) = -B_x(x,\ z),$$

$$B_z(-x,\ z) = B_z(x,\ z).$$

The electric field, that is instead a vector, transforms in the opposite way.

In both cases, in a neighborhood of a point on the z axis, taken as origin, the Taylor expansion of the magnetic field components is determined up to the second order by three parameters: a bias field B_0, which is assumed to be strictly positive, a field gradient B' and a field curvature B''.

By imposing the symmetry of case I, it is easy to show that $(\rho \equiv \sqrt{x^2+z^2})$,

$$B_x = B_0 + B'z + \frac{1}{2}B''(z^2 - x^2) + O(\rho^3), \tag{23a}$$

$$B_z = B'x + B''xz + O(\rho^3), \tag{23b}$$

whereas in case II the field is

$$B_x = -B'x - B''xz + O(\rho^3), \tag{24a}$$

$$B_z = B_0 + B'z + \frac{1}{2}B''(z^2 - x^2) + O(\rho^3). \tag{24b}$$

Each of the three parameters has a different meaning according to the symmetry case: for example, the field gradient B' is equal to $\partial B_z/\partial x$ in case I and $\partial B_z/\partial z$ in case II. Conversely, the magnetic field modulus is described by the same expression in both cases,

$$|\boldsymbol{B}| = B_0 + B'z + \frac{1}{2}B''z^2 + \frac{1}{2}\left(\frac{B'^2}{B_0} - B''\right)x^2 + O(\rho^3).$$

Concerning the electric field modulus square, by proceeding in a similar way, it follows:

$$E^2 = E_0^2 + 2E_0E'z + \frac{1}{2}(2E'^2 + 2E_0E'')z^2 + \frac{1}{2}(2E'^2 - 2E_0E'')x^2 + O(\rho^3),$$

where E_0 represents the not necessarily positive bias field, E' its gradient, and E'' its curvature.

Defining the parameters ε and ε' exactly as in Eq. (18a)–(18c), the transverse curvatures of the combined potential are expressed as follows:

$$\frac{\partial^2 U}{\partial x^2} = \mu\frac{B'^2}{2B_0}\frac{2\varepsilon - \varepsilon' - 1}{\varepsilon},$$

$$\frac{\partial^2 U}{\partial z^2} = \mu\frac{B'^2}{2B_0}\frac{\varepsilon' - 1}{\varepsilon}.$$

In analogy with the cylindrical symmetry case, we impose the y axis to coincide with the minimum of the combined confining potential described by Eq. (14). The confinement indeed occurs if

$$2E_0E' = \Gamma(B' + G),$$

$$B'' \neq 0,$$

$$2\varepsilon - 1 > \varepsilon' > 1.$$

Considerations similar to those outlined in the cylindrical symmetry case also apply in the present case. For the sake of determining size and depth of the spin-flips-free combined potential, using Eqs. (23a), (23b), (24a), and (24b), and assuming the terms of order higher than two in the Taylor expansion of the magnetic field to be negligible in a sufficiently large neighborhood of the y axis, the coordinates $(x_0,\ z_0)$ of the zeroes of the magnetic field are given by the following:

(i) $s \leq 1 \Rightarrow$

$$x_0 = 0, \quad z_0 = -\frac{B'}{B''}(1 \pm \sqrt{1-s});$$

(ii) $s \geq 1 \Rightarrow$

$$x_0 = \pm \left|\frac{B'}{B''}\right|\sqrt{s-1}, \quad z_0 = -\frac{B'}{B''};$$

where the parameter s is defined as in Eq. (18a). The zeroes correspond to two straight lines parallel to the y axis that coincide if $s=1$.

C. A translational-planar symmetric guide

Here we discuss the design of a possible combined electric-magnetic guide for rubidium atoms having $\mu=\mu_B$. Figure 2 shows the cross section. The magnetic field is generated by a standard current distribution with a current density of 10 $\mathrm{A/mm^2}$. The magnetic field lines are driven by two μ-metal pieces so as to create in the confinement region (a neighborhood of the y axis) a field directed along x and decreasing with z. This field is characterized on the y axis by a bias value of 140 G, a gradient of 1690 G/cm, and a curvature of 9610 $\mathrm{G/cm^2}$ $(s=0.94)$. In the present discussion, as the magnetic field gradient is two orders of magnitude larger than G, the role of gravity is neglected. The μ-metal can be any hysteresis-free, soft magnetic material with high permeability μ_r and saturation field B_{sat}, for example, FeCo alloys $(\mu_r \sim 1000,\ B_{\mathrm{sat}} \sim 2\ \mathrm{T})$. The maximum field occurring in the setup is about 200 G.

The magnetic configuration is covered on the top by a thin nonmagnetic end cap, which also fills out the gap between

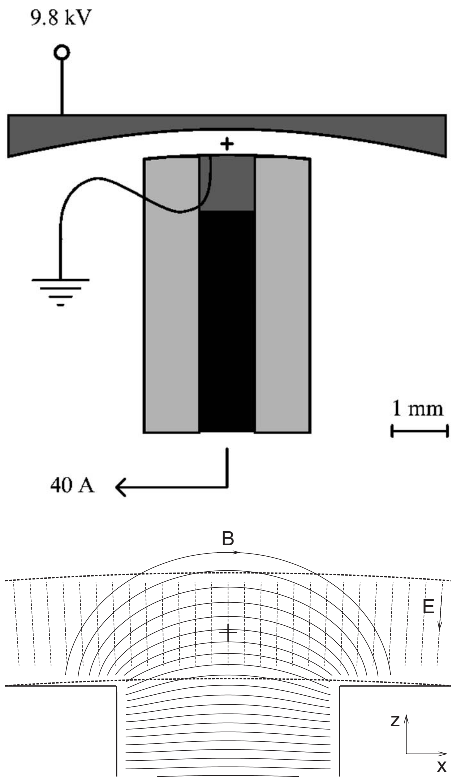

FIG. 2. Cross section (top) of a combined electric-magnetic guide for neutral atoms. The central cross corresponds to the minimum potential axis (y axis). Light gray and gray tones represent μ-metal and nonmagnetic metallic materials, respectively. The darker shade between the μ-metal pieces corresponds to a current distribution entering the page. The field lines for both magnetic (thin, continuous lines) and electric field (thin, dashed lines) are shown in the bottom cross-section view; here, the surfaces of the μ-metal elements are represented by bold, continuous lines, whereas the electrodes by bold, dashed lines.

the μ-metals. This whole bulk is grounded and, in combination with the electrode placed at +9.8 kV, generates a slightly diverging electric field characterized by a bias value of 214 kV/cm, a gradient of 140 kV/cm^2, and a curvature of 179 kV/cm^3. The parameter triplet $\{E_0, E', E''\}$ for the electric field was set on the basis of the magnetic parameters and imposing $\varepsilon = 9.3$, $\varepsilon' = 6.7$. The shape of the electrodes was then determined relying on the corresponding equipotential surfaces. All fields were calculated by means of a Galerkin finite element method [17].

The shown configuration was devised for description purposes, and is therefore not optimized. Nevertheless, it generates a steep potential (radial and axial curvature equal to 0.51 $k_B \times$ K/cm^2 and 0.72 $k_B \times$ K/cm^2, respectively). The potential is shown in Fig. 3.

It is worth remarking that with this configuration the magnetic field is everywhere nonvanishing. This feature seems to contradict the previous analysis concerning the zeroes of the magnetic field. However, the analysis above relies on the assumption that terms of order higher than two in the Taylor expansion are negligible, which does not hold in the present example.

The employment of microfabricated structures, having size of the order of 100 μm or less, and the excellent ma-

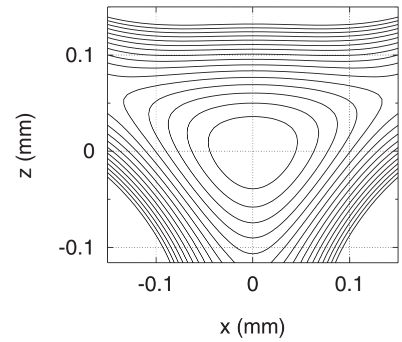

FIG. 3. Equipotential lines for the combined potential of the electric-magnetic guide of Fig. 2. The level increment between the lines is equal to 5 $k_B \times \mu$K.

chineability of several high-performance μ-metal alloys would allow for the realization of even tighter combined potentials. In this regard, it is worth remarking on the scaling behavior of the different parameters of interest (see Table II) with respect to the source size and strength.

The magnetic parameters have a less favorable dependence on the source size than the electric parameters. In conventional setups relying on current-carrying wires, this aspect is worsened by the demand of power dissipation, often resulting in a constraint on the maximum current density. These limitations could be overcome by using high-remanence permanent magnets as field sources. These materials have been employed in several experimental contexts [4,47,48]. However, their utilization implies the drawback that the generated magnetic field cannot be switched off. Concerning magnetic trapping of neutral atoms, this fact results in a major issue concerning the loading technique. On the other hand, a combined confining potential exists only if both component potentials are present; it appears then possible to devise a controllable potential by only acting on the electric field.

D. Congruent electric and magnetic fields

Finally, we discuss configurations with congruent electric and magnetic fields. Although such combination is shown to be unable to generate any confinement, the resulting potentials can be useful for other applications, such as focusing of atomic beams [49]. The role of gravity is neglected.

The electric and magnetic fields are said to be congruent if they are parallel in each point of the region of interest,

TABLE II. Dependence of bias field, gradient, and curvature on source size (r) and strength for different kinds of field sources: current I, current density J, and magnetization (remanence) M for the magnetic case; electric potential V for the electric case.

		B		E	E^2
Bias	I/r	Jr	M	V/r	V^2/r^2
Gradient	I/r^2	J	M/r	V/r^2	V^2/r^3
Curvature	I/r^3	J/r	M/r^2	V/r^3	V^2/r^4

$$\boldsymbol{E} = k\boldsymbol{B},$$

where k is a suitable proportionality factor. Congruent fields can be achieved by using μ-metal elements both to tailor the magnetic field at the confinement region and to act as electrodes.

As the gradient of the combined potential must vanish, it follows

$$2|\boldsymbol{E}_0|\boldsymbol{\gamma}_E = 2k^2|\boldsymbol{B}_0|\boldsymbol{\gamma}_B = \Gamma\boldsymbol{\gamma}_B.$$

Here, $\boldsymbol{\gamma}_B$ and $\boldsymbol{\gamma}_E$ correspond to the gradientlike vector for the two fields $\boldsymbol{B}$ and $\boldsymbol{E}$, respectively. Consequently,

$$k^2 = \frac{\Gamma}{2|\boldsymbol{B}_0|}.$$

By using these last expressions in combination with Eq. (7), the Hessian matrix of the combined potential becomes

$$\frac{\partial^2 U}{\partial r_j\, \partial r_k} = \frac{\alpha}{2}(\Gamma\xi_{B_{jk}} - 2|\boldsymbol{E}_0|\zeta_{E_{jk}}) = -\mu\frac{\gamma_{B_j}\gamma_{B_k}}{|\boldsymbol{B}_0|},$$

where ξ_B and ζ_E correspond to the Hessian matrices of $|\boldsymbol{B}|$ and $|\boldsymbol{E}|^2$, respectively. The Hessian matrix is then always nonpositive definite and thus unable to confine. However, if $\hat{\boldsymbol{z}}$ is chosen as direction of the vector $\boldsymbol{\gamma}_B$, whatever the symmetry, the combined potential becomes

$$U = -\mu\frac{|\boldsymbol{\gamma}_B|^2}{2|\boldsymbol{B}_0|}z^2.$$

In a translational-symmetric geometry where the z axis is orthogonal to the symmetry axis, this potential could be used to yield a cylindrical divergent lens for neutral particles.

VI. CONCLUSIONS

We have explored the possibility of realizing confinement systems for neutral species by using combined static potentials. A main advantage of such approach consists in a greater flexibility in designing the fields and thus in the possibility to overcome experimental constraints set by more conventional approaches.

The results presented in this paper generalize Earnshaw's theorem to linear combinations of potentials, each given by the modulus of an irrotational and solenoidal field.

Systems relying on combined potentials can be a new tool for confinement of diamagnetic species, as well as species having large electric dipole polarizabilities, such as molecules or Rydberg atoms.

This work was in part supported by the INFM Progetto di Ricerca Avanzata "photon matter."

APPENDIX: TRACE EVALUATION FOR THE CURVATURELIKE MATRICES

The demonstration of the non-negativity of the trace of the matrix ζ can be inferred by a known result concerning the Laplacian of the modulus square of a solenoidal and irrotational field (see, for example, Ref. [24]). However, we report here the demonstration as it is useful for the evaluation of the trace of the matrix ξ. The trace of the matrix ζ, as defined in Eq. (4), can be written as

$$\mathrm{Tr}\ \zeta = \frac{1}{|\boldsymbol{C}_0|}\sum_i \sum_j \left(C_{i0}\frac{\partial^2 C_i}{\partial r_j^2} + \frac{\partial C_i}{\partial r_j}\frac{\partial C_i}{\partial r_j}\right). \tag{A1}$$

As the field $\boldsymbol{C}$ is supposed to be divergence and rotation free, the Laplacian of each of its components is zero, i.e., $\nabla^2\boldsymbol{C}=0$. For this reason, the terms of Eq. (A1) containing the second derivatives cancel out. The remaining contribution is a sum of squares which can be written as

$$\mathrm{Tr}\ \zeta = \frac{1}{|\boldsymbol{C}_0|}\sum_j \frac{\partial \boldsymbol{C}}{\partial r_j}\frac{\partial \boldsymbol{C}}{\partial r_j} = \frac{1}{|\boldsymbol{C}_0|}\sum_j \left|\frac{\partial \boldsymbol{C}}{\partial r_j}\right|^2. \tag{A2}$$

It then follows that

$$\mathrm{Tr}\ \zeta \geq 0.$$

Consequently, the eigenvalues of the symmetric matrix ζ cannot be all simultaneously negative.

A similar result can be derived for the matrix ξ defined in Eq. (7): taking into account Eq. (A2), it follows that

$$\mathrm{Tr}\ \xi = \mathrm{Tr}\ \zeta - \frac{1}{|\boldsymbol{C}_0|}\sum_j \gamma_j\gamma_j,$$

and thus

$$\mathrm{Tr}\ \xi = \frac{1}{|\boldsymbol{C}_0|^3}\sum_j \left[|\boldsymbol{C}_0|^2\left|\frac{\partial \boldsymbol{C}}{\partial r_j}\right|^2 - \left(\boldsymbol{C}_0\frac{\partial \boldsymbol{C}}{\partial r_j}\right)^2\right].$$

For each j, the term in square brackets turns out to be nonnegative by virtue of the Cauchy-Schwartz inequality. Consequently,

$$\mathrm{Tr}\ \zeta \geq \mathrm{Tr}\ \xi \geq 0.$$

[1] A. L. Migdall, J. V. Prodan, W. D. Phillips, T. H. Bergeman, and H. J. Metcalf, Phys. Rev. Lett. **54**, 2596 (1985).
[2] H. Friedburg and W. Paul, Naturwiss. **38**, 159 (1951).
[3] J. Schmiedmayer, Phys. Rev. A **52**, R13 (1995).
[4] B. Ghaffari, J. M. Gerton, W. I. McAlexander, K. E. Strecker, D. M. Homan, and R. G. Hulet, Phys. Rev. A **60**, 3878 (1999).
[5] M. Key, I. G. Hughes, W. Rooijakkers, B. E. Sauer, E. A. Hinds, D. J. Richardson, and P. G. Kazansky, Phys. Rev. Lett. **84**, 1371 (2000).
[6] A. E. Leanhardt, A. P. Chikkatur, D. Kielpinski, Y. Shin, T. L. Gustavson, W. Ketterle, and D. E. Pritchard, Phys. Rev. Lett. **89**, 040401 (2002).
[7] J. Fortágh and C. Zimmermann, Rev. Mod. Phys. **79**, 235 (2007).

[8] J. D. Weinstein and K. G. Libbrecht, Phys. Rev. A **52**, 4004 (1995).
[9] M. Drndić, C. S. Lee, and R. M. Westervelt, Phys. Rev. B **63**, 085321 (2001).
[10] H. Ott, J. Fortagh, G. Schlotterbeck, A. Grossmann, and C. Zimmermann, Phys. Rev. Lett. **87**, 230401 (2001).
[11] W. Hänsel, P. Hommelhoff, T. W. Hänsch, and J. Reichel, Nature **413**, 498 (2001).
[12] D. Muller, D. Z. Anderson, R. J. Grow, P. D. D. Schwindt, and E. A. Cornell, Phys. Rev. Lett. **83**, 5194 (1999).
[13] N. H. Dekker, C. S. Lee, V. Lorent, J. H. Thywissen, S. P. Smith, M. Drndić, R. M. Westervelt, and M. Prentiss, Phys. Rev. Lett. **84**, 1124 (2000).
[14] R. Folman, P. Krüger, D. Cassettari, B. Hessmo, T. Maier, and J. Schmiedmayer, Phys. Rev. Lett. **84**, 4749 (2000).
[15] J. Reichel, W. Hansel, and T. W. Hansch, Phys. Rev. Lett. **83**, 3398 (1999).
[16] T. Nirrengarten, A. Qarry, C. Roux, A. Emmert, G. Nogues, M. Brune, J.-M. Raimond, and S. Haroche, Phys. Rev. Lett. **97**, 200405 (2006).
[17] L. Ricci, C. Zimmermann, V. Vuletić, and T. W. Hänsch, Appl. Phys. B **59**, 195 (1994).
[18] V. Vuletić, T. W. Hänsch, and C. Zimmermann, Europhys. Lett. **36**, 349 (1996).
[19] V. Vuletić, T. Fischer, M. Praeger, T. W. Hansch, and C. Zimmermann, Phys. Rev. Lett. **80**, 1634 (1998).
[20] M. Vengalattore, W. Rooijakkers, and M. Prentiss, Phys. Rev. A **66**, 053403 (2002).
[21] S. Wu, W. Rooijakkers, P. Striehl, and M. Prentiss, Phys. Rev. A **70**, 013409 (2004).
[22] W. Ketterle and D. E. Pritchard, Appl. Phys. B: Photophys. Laser Chem. **B54**, 403 (1992).
[23] C. Chin, V. Vuletić, A. J. Kerman, and S. Chu, Phys. Rev. Lett. **85**, 2717 (2000).
[24] M. V. Berry and A. K. Geim, Eur. J. Phys. **18**, 307 (1997).
[25] A. K. Geim, M. D. Simon, M. I. Boamfa, and L. O. Heflinger, Nature **400**, 323 (1999).
[26] J. Schmiedmayer, Eur. Phys. J. D **4**, 57 (1998).
[27] E. A. Hinds and I. G. Hughes, J. Phys. D **32**, R119 (1999).
[28] A. Hopkins, B. Lev, and H. Mabuchi, Phys. Rev. A **70**, 053616 (2004).
[29] P. Krüger, X. Luo, M. W. Klein, K. Brugger, A. Haase, S. Wildermuth, S. Groth, I. Bar-Joseph, R. Folman, and J. Schmiedmayer, Phys. Rev. Lett. **91**, 233201 (2003).
[30] A. E. Leanhardt, T. A. Pasquini, M. Saba, A. Schirotzek, Y. Shin, D. Kielpinski, D. E. Pritchard, and W. Ketterle, Science **301**, 1513 (2003).
[31] S. Chu, J. E. Bjorkholm, A. Ashkin, and A. Cable, Phys. Rev. Lett. **57**, 314 (1986).
[32] V. V. Klimov and V. S. Letokhov, Opt. Commun. **121**, 130 (1995).
[33] S. K. Sekatskii, B. Riedo, and G. Dietler, Opt. Commun. **195**, 197 (2001).
[34] D. Rychtarik, B. Engeser, H. C. Nagerl, and R. Grimm, Phys. Rev. Lett. **92**, 173003 (2004).
[35] M. J. Pritchard, A. S. Arnold, S. L. Cornish, D. W. Hallwood, C. V. S. Pleasant, and I. G. Hughes, New J. Phys. **8**, 309 (2006).
[36] W. H. Wing, Prog. Quantum Electron. **8**, 181 (1984).
[37] Y. Gott, M. Ioffe, and V. Tel'kovskii, Nucl. Fusion **3**, 1045 (1962).
[38] D. E. Pritchard, Phys. Rev. Lett. **51**, 1336 (1983).
[39] M. E. Gehm, K. M. O'Hara, T. A. Savard, and J. E. Thomas, Phys. Rev. A **58**, 3914 (1998).
[40] C. A. Sackett, Phys. Rev. A **73**, 013626 (2006).
[41] J. R. Yeh, B. Hoeling, and R. J. Knize, Phys. Rev. A **52**, 1388 (1995).
[42] L. Windholz, C. Krenn, G. Gwehenberger, M. Musso, and B. Schnizer, Phys. Rev. Lett. **77**, 2190 (1996).
[43] N. E. Kassimi and A. J. Thakkar, Phys. Rev. A **50**, 2948 (1994).
[44] A. Derevianko, W. R. Johnson, M. S. Safronova, and J. F. Babb, Phys. Rev. Lett. **82**, 3589 (1999).
[45] A. S. Arnold, J. Phys. B **37**, L29 (2004).
[46] S. Gupta, K. W. Murch, K. L. Moore, T. P. Purdy, and D. M. Stamper-Kurn, Phys. Rev. Lett. **95**, 143201 (2005).
[47] K. Halbach, Nucl. Instrum. Methods **169**, 1 (1980).
[48] C. C. Bradley, C. A. Sackett, J. J. Tollett, and R. G. Hulet, Phys. Rev. Lett. **75**, 1687 (1995).
[49] H.-R. Noh, K. Shimizu, and F. Shimizu, Phys. Rev. A **61**, 041601(R) (2000).